*proceedings*

MDPI

*Proceedings*

# Open Bottom Production in Au + Au Collisions at $\sqrt{s_{NN}}$ = 200 GeV with the STAR Experiment †

**Shenghui Zhang** [1,2,3]

1 Department of Modern Physics, University of Science and Technology of China (USTC), Hefei 230026, China; zhang08@ustc.edu.cn
2 Department of Radiology, Lanzhou University Second Hospital, Lanzhou 730030, China
3 Key Laboratory of Medical Imaging of Gansu Province, Lanzhou 730030, China

† Presented at Hot Quarks 2018—Workshop for young scientists on the physics of ultrarelativistic nucleus-nucleus collisions, Texel, The Netherlands, 7–14 September 2018.

Published: 24 April 2019

**Abstract:** In these proceedings, we present measurements of open bottom hadron production through multiple decay channels in Au + Au collisions at $\sqrt{s_{NN}}$ = 200 GeV by the STAR experiment. Specifically, measurements of nuclear modification factors for electrons, $J/\psi$, and $D^0$ from open bottom hadron decays, enabled by the Heavy Flavor Tracker, are shown. A large suppression for non-prompt $J/\psi$ and non-prompt $D^0$ are observed at high transverse momenta. On the other hand, there seems to be less suppression for electrons from bottom hadron decays than for those from charm hadron decays at $\sim 2\sigma$ significance level.

**Keywords:** open bottom production; nuclear modification factors; non-prompt $J/\psi$; non-prompt $D^0$; electrons from bottom hadron decays; quark-gluon plasma

## 1. Introduction

Heavy quarks are dominantly produced at early stages of relativistic heavy-ion collisions before the creation of the Quark-Gluon Plasma (QGP). They subsequently traverse the created system throughout its evolution, and thus can serve as an excellent probe for studying the properties of the QGP. By comparing the yields of electrons from decays of heavy-flavor hadrons at large transverse momenta ($p_T$) in Au + Au collisions with those in p + p collisions at $\sqrt{s_{NN}}$ = 200 GeV, a significant suppression has been observed [1]. This suppression is believed to be caused by the energy loss of heavy flavor quarks through interactions with the QGP, which is expected to be different for bottom and charm quarks because of their different masses [2]. Separate measurements of open bottom and charm hadron production in Au + Au collisions are crucial to test the mass hierarchy of parton energy loss in the QGP.

## 2. Measurements of Bottom Production at STAR

The STAR experiment utilizes the Time Projection Chamber, the Time Of Flight detector, and the Barrel Electromagnetic Calorimeter to reconstruct charged tracks and perform particle identification. The Heavy Flavor Tracker (HFT) was installed at STAR and participated in data taking from 2014 to 2016. It provides an excellent track pointing resolution (<30 μm for charged particles with $p_T >$ 1.5 GeV/c) for precise measurements of displaced vertices [3]. Therefore, the HFT can be used to separate particles from charm and bottom hadron decays by taking advantage of their different decay lengths.

### 2.1. Bottom Hadron Decay Electrons

The distance of the closest approach ($DCA$) to the collision vertex is used to separate the bottom hadron decay electrons ($B\rightarrow e$) from charm hadron decay electrons ($D\rightarrow e$). The measured $DCA$ distribution in the transverse plane ($DCA_{XY}$) for inclusive electrons is shown in the panel $(a)$ of Figure 1, along with the template fit including $B\rightarrow e$, $D\rightarrow e$, background from photonic electrons, and hadron contamination. The templates for $B\rightarrow e$ and $D\rightarrow e$ are obtained from a data-driven simulation coupled with a EvtGen [4] decayer, in which $D^0, D^{\pm}, B^0$ and $B^{\pm}$ decays are taken into account. The $DCA_{XY}$ distribution for $B\rightarrow e$ is broader than that for $D\rightarrow e$ because of the longer lifetime of B hadrons. The template for photonic electrons, arising from gamma conversions, $\pi^0$ and $\eta$ Dalitz decays, is obtained from data and corrected for the electron reconstruction efficiency extracted from embedding based on HIJING [5] simulations. Furthermore, hadrons misidentified as electron candidates need to be accounted for. Their template is obtained from data and the magnitude is constrained by the inclusive electron purity. Through the template fitting, the fraction of $B\rightarrow e$ in heavy-flavor hadron decay electrons is obtained, which is shown in the panel $(b)$ of Figure 1, along with that in p + p collisions [6]. An enhancement of the $B\rightarrow e$ fraction is observed in Au + Au collisions compared to p + p collisions.

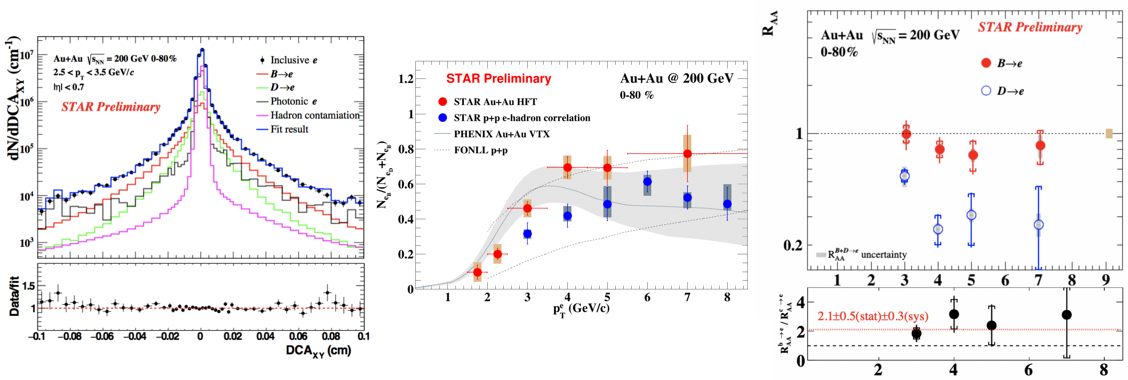


(a) (b) (c)

**Figure 1.** (**a**) $Upper$ : $DCA_{XY}$ distribution for inclusive electrons with a template fit including $B\rightarrow e$, $D\rightarrow e$, and various background sources. $Lower$ : Ratio of data to the fitted distribution. (**b**) fraction of $B\rightarrow e$ as a function of $p_T$. (**c**) $Upper$ : $R_{AA}^{B\rightarrow e}$ and $R_{AA}^{D\rightarrow e}$ as a function of $p_T$. $Lower$ : Ratio of $R_{AA}^{B\rightarrow e}$ to $R_{AA}^{D\rightarrow e}$ as a function of $p_T$.

The $R_{AA}$ of $B\rightarrow e$ and $D\rightarrow e$ are obtained using:

$$R_{AA}^{B\rightarrow e} = \frac{f_{Au+Au}^{B\rightarrow e}(data)}{f_{p+p}^{B\rightarrow e}(data)} R_{AA}^{HF_e}(data),\ R_{AA}^{D\rightarrow e} = \frac{1 - f_{Au+Au}^{B\rightarrow e}(data)}{1 - f_{p+p}^{B\rightarrow e}(data)} R_{AA}^{HF_e}(data), \quad (1)$$

where $f^{B\rightarrow e}$ is the fraction of $B\rightarrow e$ in Au + Au or p + p collisions, and $R_{AA}^{HF_e}$ is the $R_{AA}$ of open heavy-flavor hadron decay electrons obtained by taking a ratio of heavy-flavor hadron decay electron yield in Au + Au collisions to that in p + p collisions normalized by the number of binary nucleon-nucleon collisions ($N_{coll}$). In the panel $(c)$ of Figure 1, the obtained $R_{AA}^{B\rightarrow e}$, $R_{AA}^{D\rightarrow e}$ and the ratio of $R_{AA}^{B\rightarrow e}$ to $R_{AA}^{D\rightarrow e}$ in 0-80% central Au + Au collisions are shown. The $R_{AA}^{B\rightarrow e}$ is about 2.1 times larger than $R_{AA}^{D\rightarrow e}$ ($\sim 2\sigma$ significance), which is consistent with the mass hierarchy of parton energy loss.

### 2.2. Non-Prompt $J/\psi$

The pseudo-proper decay length $l_{J/\psi}$ is used to separate non-prompt and prompt $J/\psi$ and is defined as $l_{J/\psi} = \frac{\vec{L}\cdot\vec{p}}{|\vec{p}|/c} \cdot M_{J/\psi}$, where $\vec{L}$ is B hadron flight path, $\vec{p}$ the $J/\psi$ momentum, and $M_{J/\psi}$ the

$J/\psi$ mass. The $l_{J/\psi}$ distribution for inclusive $J/\psi$ is shown in the panel $(a)$ of Figure 2, along with the template fit for non-prompt and prompt $J/\psi$. The template for prompt $J/\psi$ is from FONLL calculation combined with a data-driven simulation of detector effects. For the non-prompt $J/\psi$ the template is obtained by decaying B-hadrons ($B^0$, $B^{\pm}$) from FONLL into $J/\psi$ via PYTHIA and taking into account detector effects. The fraction of non-prompt $J/\psi$ extracted from the template fit is shown in the panel $(b)$ of Figure 2, and compared to the CEM + FONLL calculation [7,8] for 200 GeV p + p collisions.

The $R_{AA}$ of non-prompt $J/\psi$ is calculated as:

$$R_{AA}^{B\to J/\psi} = \frac{f_{Au+Au}^{B\to J/\psi}(data)}{f_{p+p}^{B\to J/\psi}(theory)} R_{AA}^{inc.J/\psi}(data), \tag{2}$$

where $f^{B\to J/\psi}$ is the fraction of non-prompt $J/\psi$ in Au + Au or p + p collisions and $R_{AA}^{inc.J/\psi}$ is the $R_{AA}$ of inclusive $J/\psi$. The panel $(c)$ of Figure 2 shows the $R_{AA}$ of non-prompt $J/\psi$, together with a comparison to that of inclusive $D^0$ in 0–80% centrality of 200 GeV Au + Au collisions. A strong suppression is observed for non-prompt $J/\psi$ at high $p_T$ and is similar to that of $D^0$ mesons.

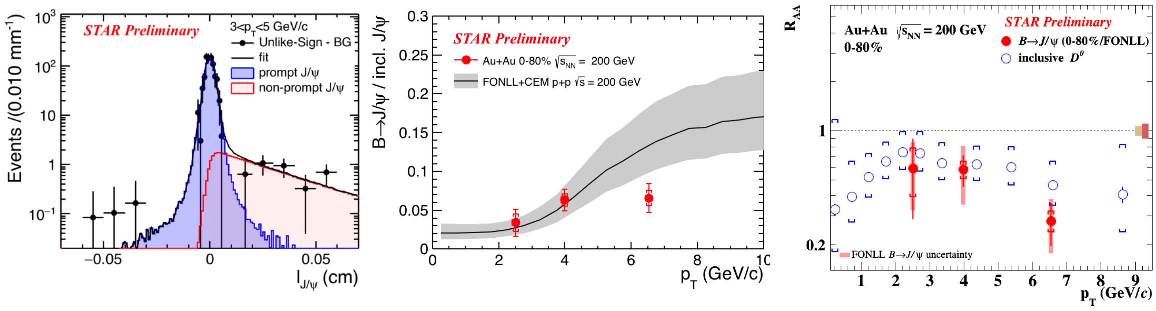


**(a)** **(b)** **(c)**

**Figure 2.** (**a**) $l_{J/\psi}$ distribution for inclusive $J/\psi$ fitted with templates for non-prompt and prompt $J/\psi$. (**b**) fraction of non-prompt $J/\psi$ as a function of $p_T$. (**c**) $R_{AA}$ of non-prompt $J/\psi$ as a function of $p_T$ compared with that of $D^0$.

### *2.3. Non-Prompt* $D^0$

The $DCA$ distribution is used to distinguish non-prompt $D^0$ from prompt ones. The panel $(a)$ of Figure 3 shows the $DCA$ distribution of inclusive $D^0$, along with the template fit of non-prompt and prompt $D^0$. The templates for non-prompt and prompt $D^0$ are obtained using the same method as for non-prompt and prompt $J/\psi$. The extracted fractions of non-prompt $D^0$ in different centralities of 200 GeV Au + Au collisions are presented in the panel $(b)$ of Figure 3. The non-prompt $D^0$ fractions in p + p collisions are also shown, which are obtained by taking a ratio of non-prompt $D^0$ yield from FONLL [8] to inclusive $D^0$ yield either from FONLL [8] or from STAR measurements [9].

The $R_{AA}$ of non-prompt $D^0$ is obtained as follows:

$$R_{AA}^{B\to D^0} = \frac{1}{< N_{coll} >} \frac{f_{Au+Au}^{B\to D^0}(data) \times dN_{Au+Au}^{inc.D^0}/dp_T(data)}{dN_{FONLL}^{B\to D^0}/dp_T(theory)}, \tag{3}$$

where $f_{Au+Au}^{B\to D^0}$ is the fraction of non-prompt $D^0$ in Au + Au collisions, $dN_{Au+Au}^{inc.D^0}/dp_T$ the inclusive $D^0$ yield in Au + Au collisions and $dN_{FONLL}^{B\to D^0}/dp_T$ the non-prompt $D^0$ yield from the FONLL calculation for p + p collisions. The panel $(c)$ of Figure 3 shows the $R_{AA}$ of non-prompt $D^0$, along with a comparison to that of inclusive $D^0$. A strong suppression of non-prompt $D^0$ is observed at high $p_T$ and there is a hint of less suppression for non-prompt $D^0$ compared to prompt ones at $4 < p_T < 6.5$ GeV/c.

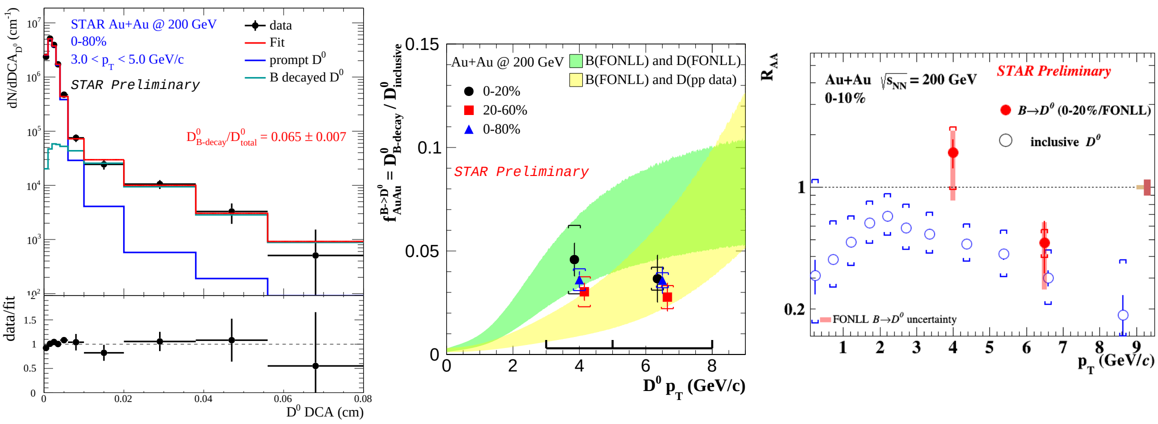


(**a**) (**b**) (**c**)

**Figure 3.** (**a**) $DCA$ distribution of inclusive $D^0$ with a template fit including non-prompt and prompt $D^0$. (**b**) fraction of non-prompt $D^0$ as a function of $p_T$ in different centralities compared to that for p + p collisions. (**c**) $R_{AA}$ of non-prompt and inclusive $D^0$ as a function of $p_T$.

## 3. Summary and Outlook

In these proceedings, we present the STAR measurements of bottom hadron production via electron, $J/\psi$, and $D^0$ decay channels in Au + Au collisions at $\sqrt{s_{\rm NN}} = 200$ GeV. For $R_{AA}$ of non-prompt $J/\psi$ and $D^0$, a strong suppression is observed at high $p_T$. For the electron channel, there is less suppression for electrons from B-hadron decays compared to those from D-hadron decays, which is consistent with the theoretical prediction that bottom quarks should lose less energy than charm quarks due to the larger bottom quark mass. Compared to the statistics used for the results presented here, a factor of $\sim 1.5$ times more minimum-bias and $\sim 5$ times more high-$p_T$ electron triggered events in 200 GeV Au + Au collisions events were recorded by the STAR experiment in 2016, which can be used to further improve the precision of the measurements for electrons and $D^0$ from B-hadron decays.

**Acknowledgments:** This work was supported in part by the Major State Basic Research Development Program in China with grant no. 2014CB845400, the National Natural Science Foundation of China with grant No. 11375184, the Youth Innovation Promotion Association fund of CAS with grant No. CX2030040079, the Science and Technological Fund of Anhui Province for Outstanding Youth with grant No. 1808085J02 and the Fundamental Research Funds for the Central Universities.

## References

1. Abelev, B.I.; Aggarwal, M.M.; Ahammed, Z.; Anderson, B.D.; Arkhipkin, D.; Averichev, G.S.; Bai, Y.; Balewski, J.; Barannikova, O.; Barnby, L.S.; et al. Transverse Momentum and Centrality Dependence of High-$p_T$ Nonphotonic Electron Suppression in Au + Au Collisions at $\sqrt{s_{\rm NN}}$ = 200 GeV. *Phys. Rev. Lett.* **2007**, *98*, 192301, doi:10.1103/PhysRevLett.98.192301.
2. Buzzatti, A.; Gyulassy, M. Jet Flavor Tomography of Quark Gluon Plasmas at RHIC and LHC. *Phys. Rev. Lett.* **2012**, *108*, 022301, doi:10.1103/PhysRevLett.108.022301.
3. Qiu, H. STAR heavy flavor tracker. *Nucl. Phys. A* **2014**, *931*, 1141–1146, doi:10.1016/j.nuclphysa.2014.08.056.
4. Lange, D.J. The EvtGen particle decay simulation package. *Nucl. Instrum. Methods Phys. Res. Sect. A Accel. Spectrometers Detect. Assoc. Equip.* **2001**, *462*, 152–155, doi:10.1016/s0168-9002(01)00089-4.
5. Wang, X.; Gyulassy, M. HIJING: A Monte Carlo model for multiple jet production in pp, pA, and AA collisions. *Phys. Rev. D* **1991**, *44*, 3501, doi:10.1103/PhysRevD.44.3501.
6. Aggarwal, M.; Ahammed, Z.; Alakhverdyants, A.; Alekseev, I.; Alford, J.; Anderson, B.; Anson, D.; Arkhipkin, D.; Averichev, G.; Balewski, J.; et al. Measurement of the Bottom Quark Contribution to Nonphotonic Electron Production in p + p Collisions at $\sqrt{s}$ = 200 GeV. *Phys. Rev. Lett.* **2010**, *105*, 202301, doi:10.1103/PhysRevLett.105.202301.
7. Frawley, A.D.; Ullrich, T.; Vogt, R. Heavy flavor in heavy-ion collisions at RHIC and RHIC II. *Phys. Rep.* **2008**, *462*, 125–175, doi:10.1016/j.physrep.2008.04.002.

8. Cacciari, M.; Frixione, S.; Nason, P. The $p_T$ Spectrum in Heavy-Flavour Photoproduction. *J. High Energy Phys.* **2001**, *2001*, 6, doi:10.1088/1126-6708/2001/03/006.
9. Adamczyk, L.; Agakishiev, G.; Aggarwal, M.M.; Ahammed, Z.; Alakhverdyants, A.V.; Alekseev, I.; Alford, J.; Anderson, B.D.; Anson, C.D.; Arkhipkin, D.; et al. Measurements of $D^0$ and $D^*$ production in p + p collisions at $\sqrt{s}$ = 200 GeV. *Phys. Rev. D* **2012**, *86*, 072013, doi:10.1103/PhysRevD.86.072013.